How to cite: *Angew. Chem. Int. Ed.* **2022**, *61*, e202117696
International Edition: doi.org/10.1002/anie.202117696
German Edition: doi.org/10.1002/ange.202117696

Carboboration **Hot Paper**

Enantio- and Diastereoselective Copper-Catalyzed Allylboration of Alkynes with Allylic *gem*-Dichlorides

*Andrea Chaves-Pouso, Andrés M. Álvarez-Constantino, and Martín Fañanás-Mastral**

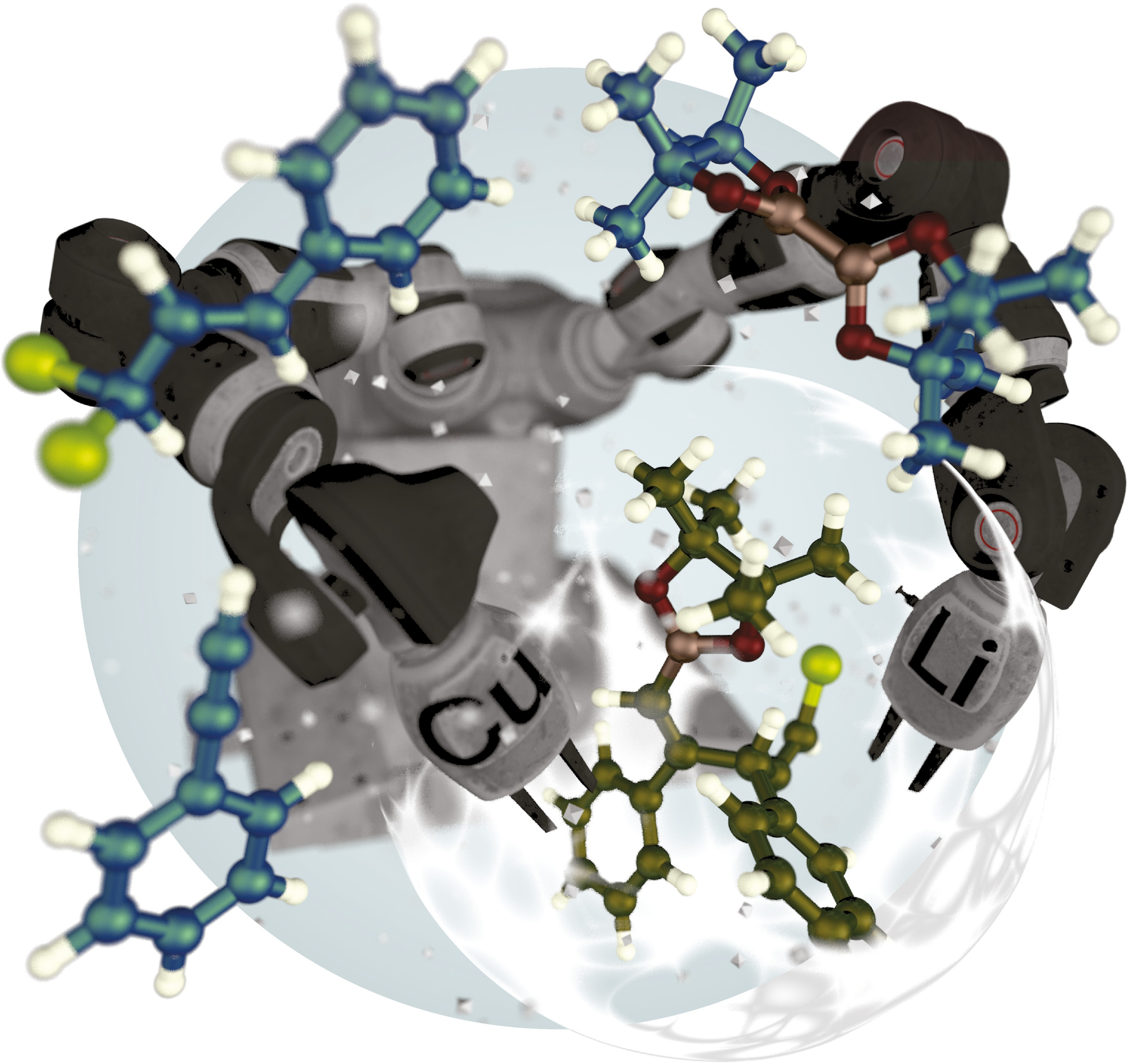

© 2022 The Authors. Angewandte Chemie International Edition published by Wiley-VCH GmbH

Abstract: Allylic *gem*-dichlorides are shown to be efficient substrates for catalytic asymmetric allylboration of alkynes. The method employs a chiral NHC–Cu catalyst capable of generating in a single step chiral skipped dienes bearing a *Z*-alkenyl chloride, a trisubstituted *E*-alkenyl boronate and a bis-allylic stereocenter with excellent levels of chemo-, regio- enantio- and diastereoselectivity. This high degree of functionalization makes these products versatile building blocks as illustrated with the synthesis of several optically active compounds. DFT calculations support the key presence of a metal cation bridge ligand–substrate interaction and account for the stereoselectivity outcome.

The presence of multiple stereochemical elements is a recurrent structural feature found in many drugs and natural products. Thus, catalytic enantioselective transformations that provide in a single operation a densely functionalized building block with several stereodefined elements in its structure are highly sought after.[1] Since pioneering studies by Hosomi and Miyaura,[2] copper-catalyzed borylative couplings of unsaturated hydrocarbons have become a powerful tool for the preparation of synthetically versatile organoboron compounds.[3] In particular, asymmetric allylboration provides access to chiral multifunctional molecules featuring both a boronic ester and an olefin group. Efficient methods either based on copper/bisphosphine[4] or synergistic Cu/Pd catalysis[5] where the stereogenic center is installed in the LCu–Bpin alkene insertion step have been reported for the allyboration of styrene derivatives (Scheme 1a). A different approach relies on the enantioselective allylic substitution of the catalytically generated organocopper intermediate, as described by Hoveyda in the borylative coupling between allenes and allylic phosphates (Scheme 1b).[6] We recently applied this strategy to the copper-catalyzed asymmetric allylboration of alkynes which involves the regio- and enantioselective coupling of an allylic bromide with a catalytically generated β-boryl-substituted alkenylcopper intermediate (Scheme 1c).[7,8] Realizing that the presence of two chlorine atoms in an allylic *gem*-dichloride might result in a dual role as leaving group and as a stereocontrol element, we envisaged that an asymmetric alkyne allylboration reaction based on this type of allylic substrates might lead to an unprecedented degree of complexity in which two new stereodefined olefins and a bis-allylic stereocenter would be created in a single step (Scheme 1d). The products of this transformation would bear two orthogonal functionalities, an alkenyl boronate and an alkenyl chloride, which offer diverse possibilities for the functionalization of the important skipped diene core.[9] Such a process represents a formidable challenge since diastereoselective formation of the alkenyl chloride must be achieved besides control over the chemo-, regio- and enantioselectivity. It is important to note that copper-catalyzed enantioselective allylic substitution (EAS) has been mainly applied to primary allylic substrates for the synthesis of terminal olefins,[10,11] and processes involving acyclic secondary 1,1-disubstituted allylic substrates are rare. Indeed, the use of this type of substrates in copper-catalyzed EAS has been limited to the introduction of alkyl Grignard compounds,[12] and the control over the geometry of the resulting internal double bond represents a major issue.

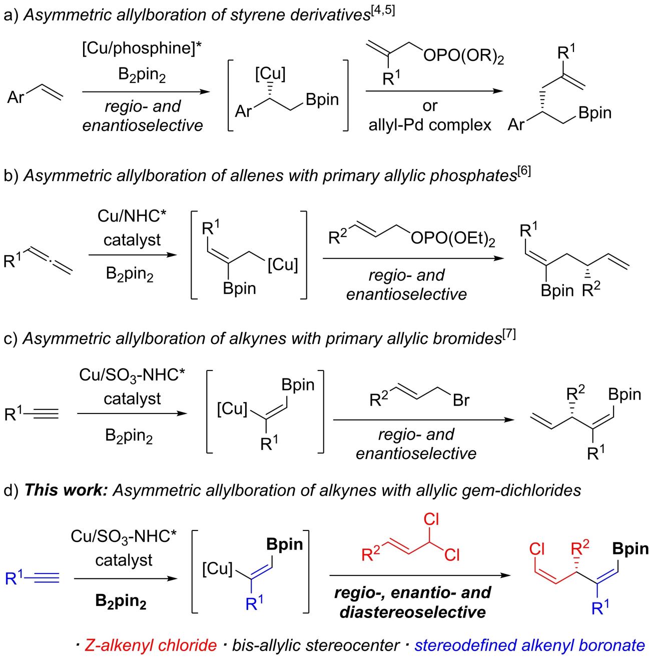
a) *Asymmetric allylboration of styrene derivatives*[4,5]

b) *Asymmetric allylboration of allenes with primary allylic phosphates*[6]

c) *Asymmetric allylboration of alkynes with primary allylic bromides*[7]

d) ***This work:*** *Asymmetric allylboration of alkynes with allylic gem-dichlorides*

· Z-alkenyl chloride · bis-allylic stereocenter · stereodefined alkenyl boronate

Scheme 1. Copper-catalyzed enantioselective allylboration of unsaturated hydrocarbons.

Herein we describe the successful use of allylic *gem*-dichlorides in a copper-catalyzed asymmetric borylative coupling with alkynes which efficiently provides chiral densely functionalized skipped dienes bearing a *Z*-alkenyl chloride and a trisubstituted stereodefined alkenyl boronate. The fact that C–C and C–B bond formation is achieved with high chemo-, regio-, enantio- and diastereoselectivity while establishing one stereocenter and two stereodefined internal olefins makes this method significant and distinct from previous copper-catalyzed carboboration and EAS reactions. Moreover, it represents a new synthetic approach among the few catalytic methods available for the stereoselective synthesis of acyclic 1,2-disubstituted alkenyl chlorides.[13]

---

[*] A. Chaves-Pouso, A. M. Álvarez-Constantino,
Prof. M. Fañanás-Mastral
Centro Singular de Investigación en Química Biolóxica e Materiais Moleculares (CiQUS), Departamento de Química Orgánica, Universidade de Santiago de Compostela
15782 Santiago de Compostela (Spain)
E-mail: martin.fananas@usc.es

© 2022 The Authors. Angewandte Chemie International Edition published by Wiley-VCH GmbH. This is an open access article under the terms of the Creative Commons Attribution Non-Commercial NoDerivs License, which permits use and distribution in any medium, provided the original work is properly cited, the use is non-commercial and no modifications or adaptations are made.

© 2022 The Authors. Angewandte Chemie International Edition published by Wiley-VCH GmbH

We began our study by exploring the reaction between phenylacetylene **1**, (*E*)-(3,3-dichloroprop-1-en-1-yl)benzene **2** and B_2pin_2 (Table 1). In our previous work on the copper-catalyzed enantioselective alkyne allylboration with allylic bromides,[7] we found that the use of a chiral sulfonate-bearing NHC ligand[14] was key to control the selectivity of the process by establishing a metal cation bridge interaction between the copper complex and the allylic bromide. Thus, we envisaged that this type of supramolecular interaction might be also crucial to control both the enantioselectivity and the diastereoselective formation of the resulting alkenyl chloride in the reaction with an allylic *gem*-dichloride. Indeed, the use of other types of chiral bisphosphine or NHC ligands led to nearly equimolar mixtures of dienes **3-*E,Z*** and **3-*E,E*** in low yield with negligible enantioselectivity (entries 1–3).According to our hypothesis, a major increase both in efficiency and selectivity was observed when sulfonate-bearing NHC ligands were employed. By using NaO^{t}Bu as base and toluene as solvent, the chiral Cu catalyst derived from ligand **L4** which features a NMes unit provided diene **3-*E,Z*** as the major isomer (*E/Z*:*E/E*= 84:16) with a very good enantioselectivity (97:3 er) (entry 4). Interestingly, the use of ligand **L5** bearing a slightly less bulky 2,6-dimethyl substituted aryl ring led to a similar result with an improved 99:1 enantiomeric ratio (entry 5). In contrast, the use of ligands with bulkier aryl groups resulted in diminished conversion and selectivity (entry 6). Evaluation of different bases and solvents using **L5** as ligand highlighted the important role of the base metal cation. A significant drop in selectivity was observed when KO^{t}Bu was used (entry 7). In contrast, product **3-*E,Z*** was almost exclusively obtained with excellent enantiomeric ratio by using LiO^{t}Bu (entry 8). Low conversion and a slight decrease in selectivity were observed when a less polar solvent such as hexane was used (entry 9). Full conversion was recovered with the more polar solvent THF, although it caused a change in selectivity affording product **3-*E,E*** as the major isomer, although as a nearly racemic mixture (entry 10). Gratifyingly, the use of ligand **L4** under the best set of conditions (LiO^{t}Bu as base and toluene as solvent) led to the exclusive formation of product **3-*E,Z*** with perfect enantioselectivity (entry 11). X-ray diffraction analysis of **3-*E,Z*** revealed the relative and absolute stereochemistry of the product.[15]

Table 1: Optimization studies.

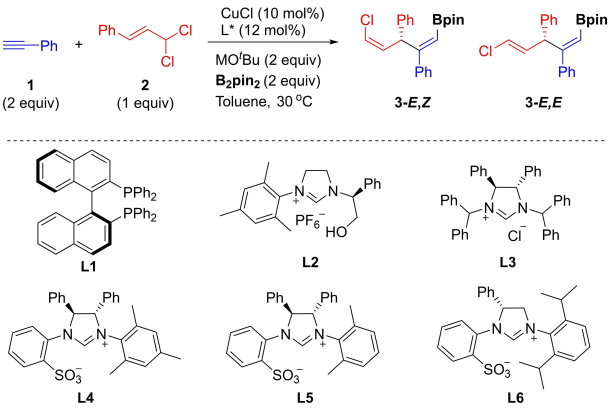

Entry[a]	L*	M	Conv. [%][b]	*E,Z/E,E* ratio[c]	**3** (*E,Z/E,E*) yield [%][d]	**3** (*E,Z/E,E*) er[e]
1	**L1**	Na	21	n.d.[f]	4/12	57:43/53:47
2	**L2**	Na	40	41:59	12/24	54:46/50:50
3	**L3**	Na	23	n.d.[f]	4/13	56:44/49:51
4	**L4**	Na	84	84:16	51/13	97:3/49:51
5	**L5**	Na	88	85:15	64/12	99:1/57:43
6	**L6**	Na	44	78:22	20/8	7:93/47:53
7	**L5**	K	76	82:18	37/12	92:8/49:51
8	**L5**	Li	Full	92:8	67/6	99:1/50:50
9[g]	**L5**	Li	16	84:16	10/2	97:3/49:51
10[h]	**L5**	Li	Full	23:77	18/69	82:18/46:54
11	**L4**	Li	Full	99:1	74/–	>99:1/–

[a] Reaction conditions: **1** (0.4 mmol), **2** (0.2 mmol), B_2pin_2 (0.4 mmol), CuCl (10 mol%), ligand (12 mol%), base (0.4 mmol), solvent (1.5 mL) at 30 °C. [b] Conversion (**2** consumption) was determined by ^1H NMR analysis using trimethyl benzene 1,3,5-tricarboxylate as internal standard. [c] Determined by GC analysis of reaction crude. [d] Yield of isolated product. [e] Enantioselectivity determined by SFC analysis. [f] n.d. = not determined. Minor diastereomer could not be detected by GC analysis. [g] Hexane used instead of toluene. [h] THF used instead of toluene.

Having established optimized conditions, we set out to explore the scope of the reaction (Scheme 2). The Cu/**L4** catalyst proved to be remarkably effective with a range of alkynes and allylic *gem*-dichlorides,[16] with **L5** giving slightly superior results in some cases. Difunctional skipped *E*,*Z*-dienes were obtained in good yields and with excellent regio-, enantio- and diastereoselectivity in nearly all cases. Aryl alkynes with electron-donating groups were well tolerated and provided dienes **4–6** as pure homochiral products. Similarly, alkynes bearing electron-withdrawing groups such as halogen (**7**, **8**) and ester (**9**) substituents also performed well, although they proved to be less reactive and required higher temperatures. The reaction also proceeded efficiently with alkynes featuring heterocyclic (**10–11**) and cyclopropyl (**12**) rings or a conjugated double bond (**13**). The use of acyclic alkyl-substituted alkynes led to diminished yields, although corresponding products **14** and **15** were still obtained with high regio-, enantio- and diastereocontrol. Importantly, as illustrated by the synthesis of diene **3**, the reaction could be scaled up to 2 mmol using lower catalyst loading (5 mol %) without any loss in yield or selectivity.

Allylic *gem*-dichlorides with aryl groups bearing different substituents at the *ortho*-, *meta*- and *para*-positions were also well tolerated and provided the corresponding chiral dienes **16–20** in good yield with excellent selectivities. Only a slight decrease in the diastereoselectivity was observed when an *ortho*-bromo substituted substrate was used. A substrate featuring a sterically demanding naphthalene group could also be used with very high selectivity (**21**). Notably, allylic *gem*-dichlorides bearing aliphatic substituents were also efficient partners in this transformation. Despite being used as a mixture of 1,1- and 1,3-isomers,[17] these substrates provided the corresponding skipped dienes **22** and **23** in good yield and with excellent selectivity. Interestingly, an allylic *gem*-dichloride derived from (−)-

© 2022 The Authors. Angewandte Chemie International Edition published by Wiley-VCH GmbH

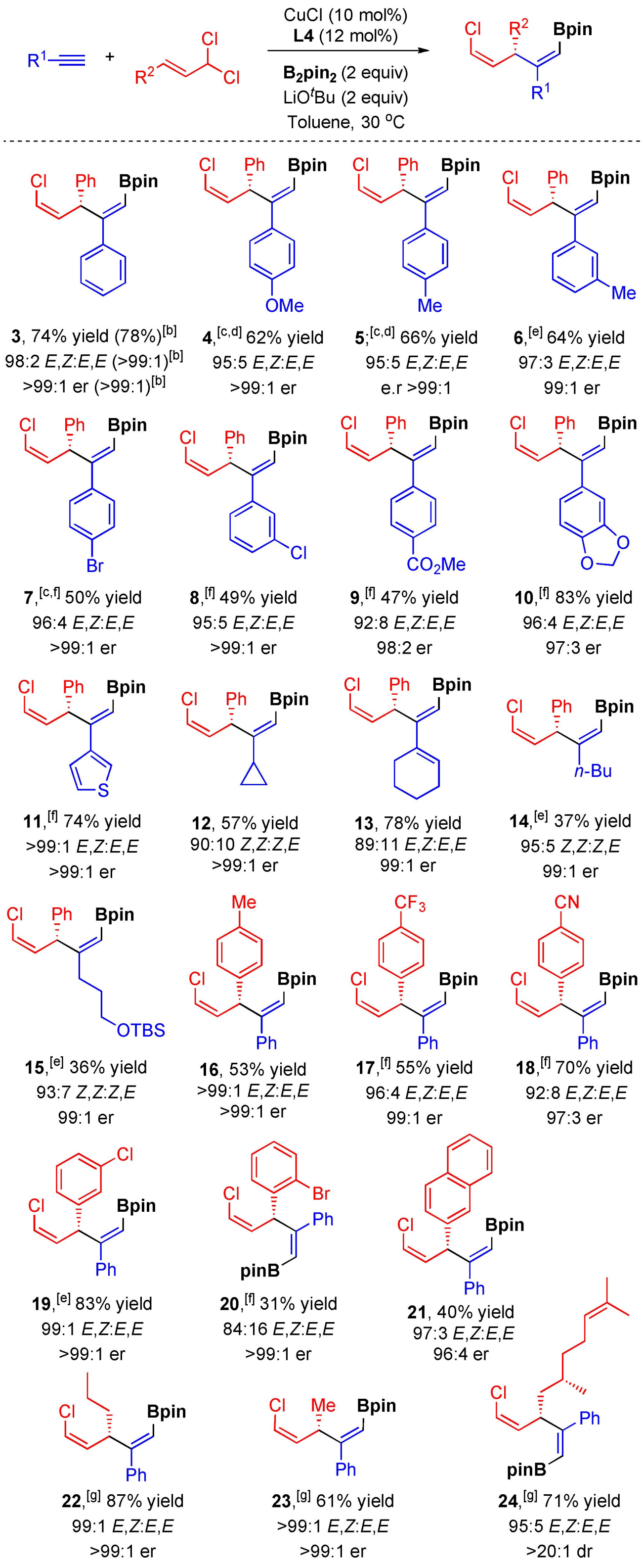

Scheme 2. Scope of the reaction. [a] Reaction conditions: see Table 1, entry 11. Yield values refer to isolated products. [b] Reaction run on a 2 mmol scale using 5 mol% of catalyst. [c] **L5** was used instead **L4**. [d] At 40 °C. [e] At 50 °C. [f] At 60 °C. [g] Obtained from a 0.8 : 1 mixture of the allylic 1,1- and 1,3-dichlorides. Yield is referred to the 1,1-isomer.

citronellal which bears an extra double bond and a stereogenic center could be used with complete levels of chemo- and diastereoselectivity (**24**).

The presence of two orthogonal functionalities at both termini of the products offers a versatile synthetic handle for further chemoselective functionalization (Scheme 3). Different stereodefined chiral skipped dienes could be accessed by Suzuki cross-coupling (**25**), Matteson homologation/oxidation (**26**) or a sequential combination of both (**27**). Notably, subsequent treatment of **23** with β-bromostyrene and 1-octenyl boronic acid under palladium catalysis afforded skipped tetraene **29**. Few methods for the synthesis of these compounds have been reported[18] and, to the best of our knowledge, examples of chiral enantioenriched skipped tetraenes are elusive.

To rationalize the high levels of enantio- and diastereoselectivity, DFT calculations were performed (see the Supporting Information for details). Optimized structures for the stereochemistry-determining S_N2'-type oxidative addition step[19,20] show that the allylic *gem*-dichloride approaches the alkenylcopper intermediate opposite to the sizable *N*-aryl group while establishing a lithium cation bridge interaction between the NHC's sulfonate group and one (or both) of the chloride units (Figure 1a). Comparison between transition states $\mathbf{TS_{OA}}$-***Z,R*** and $\mathbf{TS_{OA}}$-***Z,S*** shows that the former is favored by 9.0 kcal mol^{-1} and suggests that the origin of enantioselectivity arises from the repulsive steric interaction that is engendered between the Bpin unit and the phenyl substituent of the allylic substrate in transition state $\mathbf{TS_{OA}}$-***Z,S*** leading to the minor *S* enantiomer. A similar model may apply for the transition states associated to the formation of the minor *E,E*-isomer (Fig-

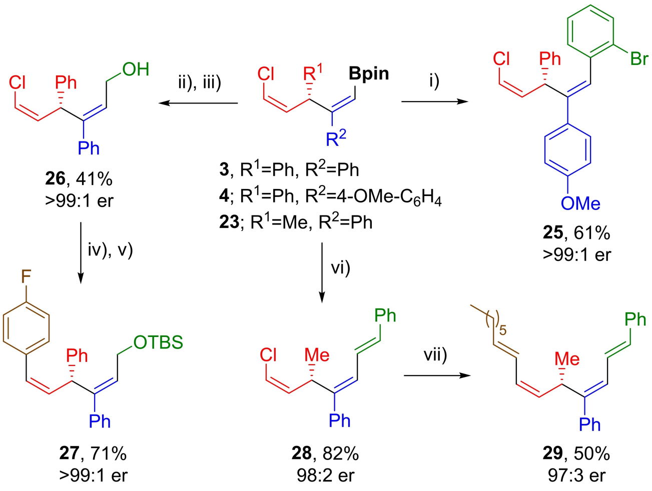

Scheme 3. Synthetic modifications of products. Conditions: i) 1-bromo-2-iodobenzene (1.5 equiv), Pd(PPh)$_3$ (10 mol%), NaOH 2 M, dioxane, 100 °C; ii) CH_2Br_2 (2 equiv), *n*-BuLi (0.5 equiv), THF, −78 °C to rt; iii) $NaBO_3\cdot 4H_2O$ (5 equiv), H_2O, rt; iv) TBSCl (1.2 equiv), imidazole (2 equiv), CH_2Cl_2, rt; v) 4-fluorophenylboronic acid (1.5 equiv), $Pd_2(dba)_3$ (5 mol%), XPhos (10 mol%), CsF (3 equiv), dioxane, 100 °C; vi) β-bromostyrene (1.5 equiv), NaOH 2 M, dioxane, 100 °C; vii) 1-octenyl boronic acid (1.5 equiv), $Pd_2(dba)_3$ (5 mol%), XPhos (10 mol%), dioxane, 100 °C.

© 2022 The Authors. Angewandte Chemie International Edition published by Wiley-VCH GmbH

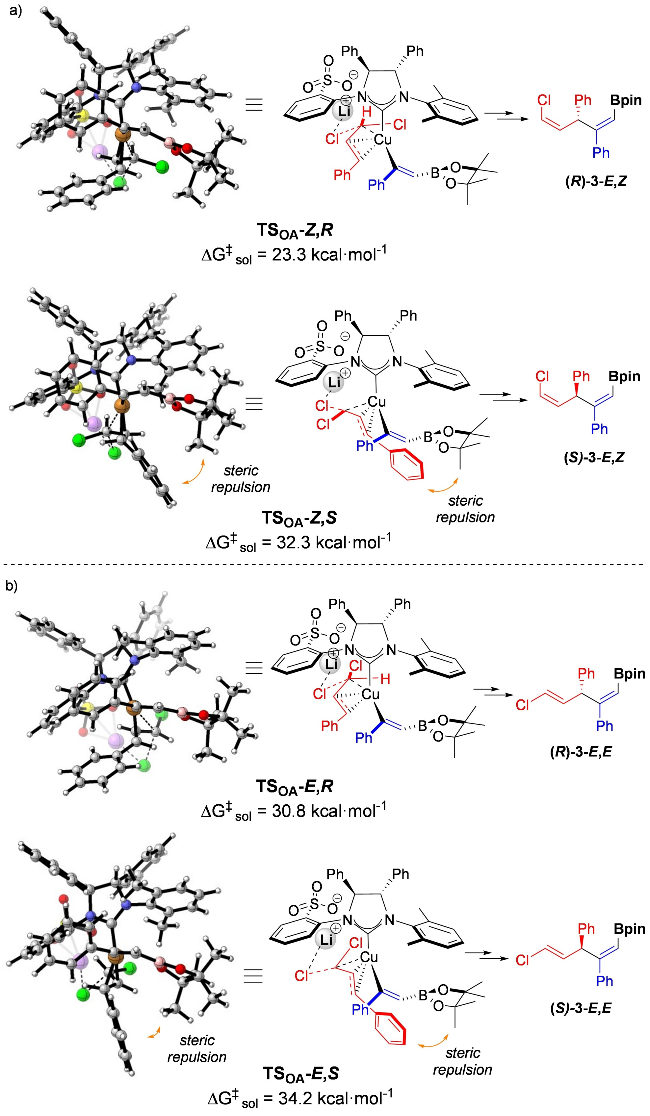

Figure 1. Optimized structures and energies for the stereochemistry-determining oxidative addition transition states obtained from DFT calculations performed at the ωB97XD/Def2-TZVPP$_{\mathrm{tol(SMD)}}$//ωB97XD/6-31G(d) level.

ure 1b). In accordance with the experimental results, both **TS$_{OA}$-*E*,*R*** and **TS$_{OA}$-*E*,*S*** resulted higher in energy than the preferred **TS$_{OA}$-*Z*,*R***.

Another important aspect to elucidate was the effect of the metal cation in the diastereoselective formation of the *Z*-alkenyl chloride. Analysis of structures for **TS$_{OA}$-Z,*R*** and **TS$_{OA}$-*E*,*R*** (Figure 2a) shows that the lithium bridge imposes a bigger $\mathrm{C_{NHC}}$–Cu–$\mathrm{C_{\alpha}}$ angle in **TS$_{OA}$-*E*,*R*** (99.9° versus 93.0° in **TS$_{OA}$-Z,*R***). This angle opening pushes the allyl substrate closer to the Bpin unit leading to a larger repulsive interaction. Calculations using sodium instead of lithium (Figure 2b) showed that this cation causes a similar enlargement of the $\mathrm{C_{NHC}}$–Cu–$\mathrm{C_{\alpha}}$ angle in **TS$_{OA}$-*E*,*R*-Na** with respect to **TS$_{OA}$-Z,*R*-Na** (101.5° versus 92.0°).[21] Distortion-interaction analysis[22,23] of the stereodeterminig transition states helped to gather insight about the different results obtained with these two metal cations. These studies revealed that **TS$_{OA}$-*E*,*R*** distortion energy ($\Delta\Delta E^{\ddagger}_{\mathrm{dist}}$) is 13.7 kcal mol^{-1} higher than **TS$_{OA}$-Z,*R***, while interaction energy ($\Delta\Delta E^{\ddagger}_{\mathrm{int}}$) only favors **TS$_{OA}$-*E*,*R*** by 5.3 kcal mol^{-1} (Figure 2a). Distortion energy of **TS$_{OA}$-*E*,*R*-Na** related to **TS$_{OA}$-Z,*R*-Na** ($\Delta\Delta E^{\ddagger}_{\mathrm{dist}}=13.9$ kcal mol^{-1}) is comparable with the value observed for the transition states featuring a lithium cation. However, stabilizing interaction energy is significantly higher for the sodium-based system ($\Delta\Delta E^{\ddagger}_{\mathrm{int}}=-9.1$ kcal mol^{-1}), thus resulting in a lower energy difference between both sodium-based transition states (Figure 2b). The increase in the stabilizing interaction energy may be due to the larger size of the Na cation which might facilitate a more effective interaction with both chlorine atoms. This might explain the slightly lower *Z*/*E* selectivity observed when NaO^{t}Bu is used instead of LiO^{t}Bu.

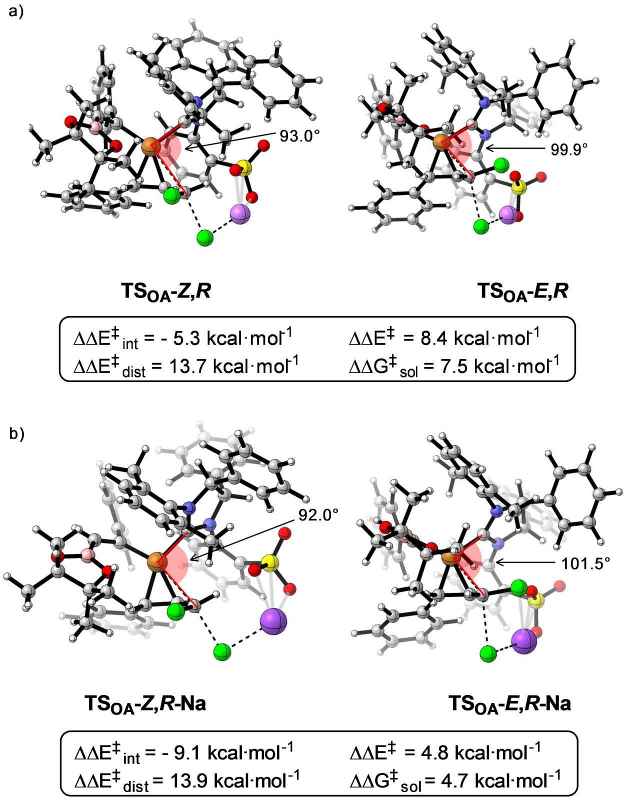

Figure 2. Optimized structures (back view) for the stereochemistry-determining oxidative addition transition states associated with the pathways leading to *R*,*E*,*Z* and *R*,*E*,*E* isomers using a) LiO^{t}Bu and b) NaO^{t}Bu. DFT calculations were performed at the ωB97XD/Def2-TZVPP$_{\mathrm{tol(SMD)}}$//ωB97XD/6-31G(d) level. Energies from distortion–interaction analysis (DIA) are referenced to the corresponding **TS$_{OA}$-Z,*R*** in each pair.

A different mechanistic scenario may apply when THF is used as solvent. Its more polar and coordinating nature may weaken (or disrupt) the supramolecular cation bridging ligand-substrate interaction leading to a looser transition state, which would result in an enantioselectivity drop and the preferential formation of the *E*-alkenyl chloride (Table 1, entry 10), as it happens when other NHC ligands

© 2022 The Authors. Angewandte Chemie International Edition published by Wiley-VCH GmbH

lacking the sulfonate group are used (Table 1, entries 2 and 3).

In conclusion, we have developed a highly chemo-, regio-, enantio- and diastereoselective coupling of alkynes, diborons and allylic *gem*-dichlorides. The use of this new class of allylic substrates for asymmetric copper-catalyzed carboboration provides chiral orthogonally functionalized skipped dienes which serve as highly versatile optically active building blocks for asymmetric synthesis. Intrinsic features of the mechanism could be unveiled by DFT calculations, showcasing the crucial role of a lithium cation bridge ligand–substrate interaction as a key stereocontrol element.

Acknowledgements

Financial support from the AEI (PID2020-118237RB-I00), Xunta de Galicia (ED431C 2018/04; Centro singular de investigación de Galicia accreditation 2019–2022, ED431G 2019/03) and the European Union (European Regional Development Fund - ERDF) is gratefully acknowledged. A. M. A.-C. thanks Xunta de Galicia for a predoctoral fellowship. We also thank the use of RIAIDT-USC analytical facilities and CESGA (Xunta de Galicia) for computational time.

Conflict of Interest

The authors declare no conflict of interest.

Data Availability Statement

The data that support the findings of this study are available in the supplementary material of this article.

Keywords: Asymmetric Catalysis · Carboboration · Copper · *gem*-Dichlorides · Skipped Dienes

---

[1] a) C. de Graaff, E. Ruijter, R. V. A. Orru, *Chem. Soc. Rev.* **2012**, *41*, 3969–4009; b) P. S. Gonçalves Nunes, H. D. Almeida Vidal, A. G. Corrêa, *Org. Biomol. Chem.* **2020**, *18*, 7751–7773.

[2] a) H. Ito, H. Yamanaka, J. Tateiwa, A. Hosomi, *Tetrahedron Lett.* **2000**, *41*, 6821–6825; b) K. Takahashi, T. Ishiyama, N. Miyaura, *J. Organomet. Chem.* **2001**, *625*, 47–53.

[3] For reviews see: a) K. Semba, T. Fujihara, J. Terao, Y. Tsuji, *Tetrahedron* **2015**, *71*, 2183–2197; b) H. Yoshida, *ACS Catal.* **2016**, *6*, 1799–1811; c) D. Hemming, R. Fritzemeier, S. A. Westcott, W. L. Santos, P. G. Steel, *Chem. Soc. Rev.* **2018**, *47*, 7477–7494; d) A. Whyte, A. Torelli, B. Mirabi, A. Zhang, M. Lautens, *ACS Catal.* **2020**, *10*, 11578–11622; e) F. J. T. Talbot, Q. Dherbassy, S. Manna, C. Shi, S. Zhang, G. P. Howell, G. J. P. Perry, D. J. Procter, *Angew. Chem. Int. Ed.* **2020**, *59*, 20278–20289; *Angew. Chem.* **2020**, *132*, 20454–20465.

[4] a) N. Kim, J. T. Han, D. H. Ryu, J. Yun, *Org. Lett.* **2017**, *19*, 6144–6147; b) J. Lee, S. Radomkit, S. Torker, J. del Pozo, A. H. Hoveyda, *Nat. Chem.* **2018**, *10*, 99–108.

[5] T. Jia, P. Cao, B. Wang, Y. Lou, X. Yin, M. Wang, J. Liao, *J. Am. Chem. Soc.* **2015**, *137*, 13760–13763.

[6] F. Meng, K. P. McGrath, A. H. Hoveyda, *Nature* **2014**, *513*, 367–374.

[7] E. Rivera-Chao, M. Mitxelena, J. A. Varela, M. Fañanás-Mastral, *Angew. Chem. Int. Ed.* **2019**, *58*, 18230–18234; *Angew. Chem.* **2019**, *131*, 18398–18402.

[8] For related non-enantioselective reactions see: a) H.-Y. Bin, X. Wei, J. Zi, Y.-J. Zuo, T.-C. Wang, C.-M. Zhong, *ACS Catal.* **2015**, *5*, 6670–6679; b) H. Jing, X. Feng, M. Guo, S. Zhou, Y. Li, J. Zhang, W. Zhao, X. Tang, G. Wang, *Asian J. Org. Chem.* **2017**, *6*, 1375–1379; c) J. Mateos, E. Rivera-Chao, M. Fañanás-Mastral, *ACS Catal.* **2017**, *7*, 5340–5344; d) E. Rivera-Chao, M. Fañanás-Mastral, *Angew. Chem. Int. Ed.* **2018**, *57*, 9945–9949; *Angew. Chem.* **2018**, *130*, 10093–10097.

[9] a) M. C. Wilson, S.-J. Nam, T. A. M. Gulder, C. A. Kauffman, P. R. Jensen, W. Fenical, B. S. Moore, *J. Am. Chem. Soc.* **2011**, *133*, 1971–1977; b) Y. Huang, M. Fañanás-Mastral, A. J. Minnaard, B. L. Feringa, *Chem. Commun.* **2013**, *49*, 3309–3311; c) T. Sato, T. Suto, Y. Nagashima, S. Mukai, N. Chida, *Asian J. Org. Chem.* **2021**, *10*, 2486–2502; d) G. Petruncio, Z. Shellnutt, S. Elahi-Mohassel, S. Alishetty, M. Paige, *Nat. Prod. Rep.* **2021**, *38*, 2187–2213.

[10] a) A. Alexakis, J. E. Bäckvall, N. Krause, O. Pàmies, M. Diéguez, *Chem. Rev.* **2008**, *108*, 2796–2823; b) S. Harutyunyan, T. Den Hartog, K. Geurts, A. J. Minnaard, B. L. Feringa, *Chem. Rev.* **2008**, *108*, 2824–2852; c) O. Baslé, A. Denicourt-Nowicki, C. Crévisy, M. Mauduit, in *Copper-Catalyzed Asymmetric Synthesis* (Eds.: A. Alexakis, N. Krause, S. Woodward), Wiley-VCH, Weinheim, **2014**, pp. 85–125.

[11] For copper-catalyzed enantioselective allylic substitution with cyclic secondary allylic substrates, see: a) J. B. Langlois, D. Emery, J. Mareda, A. Alexakis, *Chem. Sci.* **2012**, *3*, 1062–1069; b) H. You, E. Rideau, M. Sidera, S. P. Fletcher, *Nature* **2015**, *517*, 351–355; c) S. S. Goh, S. Guduguntla, T. Kikuchi, M. Lutz, E. Otten, M. Fujita, B. L. Feringa, *J. Am. Chem. Soc.* **2018**, *140*, 7052–7055; d) R. Jacques, R. D. C. Pullin, S. P. Fletcher, *Nat. Commun.* **2019**, *10*, 21.

[12] a) M. Fañanás-Mastral, B. L. Feringa, *J. Am. Chem. Soc.* **2010**, *132*, 13152–13153; b) J. B. Langlois, A. Alexakis, *Angew. Chem. Int. Ed.* **2011**, *50*, 1877–1881; *Angew. Chem.* **2011**, *123*, 1917–1921; c) M. Giannerini, M. Fañanás-Mastral, B. L. Feringa, *J. Am. Chem. Soc.* **2012**, *134*, 4108–4111.

[13] M. Joo Koh, T. T. Nguyen, H. Zhang, R. R. Schrock, A. H. Hoveyda, *Nature* **2016**, *531*, 459–465.

[14] For a review on the use of sulfonate-bearing NHC–Cu complexes in enantioselective catalysis, see: a) A. H. Hoveyda, Y. Zhou, Y. Shi, M. K. Brown, H. Wu, S. Torker, *Angew. Chem. Int. Ed.* **2020**, *59*, 21304–21359; *Angew. Chem.* **2020**, *132*, 21488–21543. For selected examples, see: b) F. Gao, J. L. Carr, A. H. Hoveyda, *J. Am. Chem. Soc.* **2014**, *136*, 2149–2161; c) Y. Shi, B. Jung, S. Torker, A. H. Hoveyda, *J. Am. Chem. Soc.* **2015**, *137*, 8948–8964; d) Y. Zhou, Y. Shi, S. Torker, A. H. Hoveyda, *J. Am. Chem. Soc.* **2018**, *140*, 16842–16854; e) Y. Sun, Y. Zhou, Y. Shi, J. del Pozo, S. Torker, A. H. Hoveyda, *J. Am. Chem. Soc.* **2019**, *141*, 12087–12099.

[15] Deposition number 2128286 contains the supplementary crystallographic data for this paper. These data are provided free of charge by the joint Cambridge Crystallographic Data Centre and Fachinformationszentrum Karlsruhe Access Structures service.

[16] Allylic *gem*-dichlorides are readily obtained from the corresponding α,β-unsaturated aldehyde by reaction with $SOCl_2$ or oxalyl chloride (see the Supporting Information for details).

[17] Allylic 1,3-dichlorides seemed not to participate in the reaction and were recovered with partial decomposition. For the synthesis of products **22** and **24**, the corresponding allylic 1,3-

dichloride were recovered in 37 % and 99 %, respectively. In case of product **23**, the 1,3-dichloride could not be recovered likely due to volatility issues.

[18] a) H. N. Lim, K. A. Parker, *J. Am. Chem. Soc.* **2011**, *133*, 20149–20151; b) A. Schmidt, G. Hilt, *Org. Lett.* **2013**, *15*, 2708–2711; c) G. I. A. Deiab, M. H. Al-Huniti, I. F. D. Hyatt, E. E. Nagy, K. E. Gettys, S. S. Sayed, C. M. Joliat, P. E. Daniel, R. M. Vummalaneni, A. T. Morehead Jr, A. L. Sargent, M. P. Croatt, *Beilstein J. Org. Chem.* **2017**, *13*, 384–392.

[19] N. Yoshikai, E. Nakamura, *Chem. Rev.* **2012**, *112*, 2339–2372.

[20] For the whole reaction energy profiles see the Supporting Information.

[21] Non-covalent interaction plots of the related transition states support this type of repulsive interactions. For further details see the Supporting Information.

[22] a) K. Morokuma, *J. Chem. Phys.* **1971**, *55*, 1236–1244; b) F. M. Bickelhaupt, *J. Comput. Chem.* **1999**, *20*, 114–128; c) D. H. Ess, K. N. Houk, *J. Am. Chem. Soc.* **2007**, *129*, 10646–10647; d) S. Gao, M. Duan, J. Liu, P. Yu, K. N. Houk, M. Chen, *Angew. Chem. Int. Ed.* **2021**, *60*, 24096–24106; *Angew. Chem.* **2021**, *133*, 24298–24308. For a tutorial review, see: e) F. M. Bickelhaupt, K. N. Houk, *Angew. Chem. Int. Ed.* **2017**, *56*, 10070–10086; *Angew. Chem.* **2017**, *129*, 10204–10221.

[23] Energy differences ($\Delta\Delta E^{\ddagger}$) between each pair of transition states were divided into contributions from the distortions of both the NHC–Cu-alkenylboronate and the allylic *gem*-dichloride into the transition state structures ($\Delta\Delta E^{\ddagger}_{\text{dist}}$), and the contributions in noncovalent interactions between the NHC–Cu-alkenylboronate and the allylic *gem*-dichloride ($\Delta\Delta E^{\ddagger}_{\text{int}}$). See Supporting Information for details.

Manuscript received: December 27, 2021
Accepted manuscript online: March 9, 2022
Version of record online: March 21, 2022

© 2022 The Authors. Angewandte Chemie International Edition published by Wiley-VCH GmbH